CD31 signals confer immune privilege to the vascular endothelium.

Cheung, K; Ma, L; Wang, G; Coe, D; Ferro, R; Falasca, M; Buckley, CD; Mauro, C; Marelli-Berg, FM

2016 National Academy of Sciences.

For additional information about this publication click this link.
http://qmro.qmul.ac.uk/xmlui/handle/123456789/18146

CD31 signals confer immune privilege to the vascular endothelium

Kenneth Cheung[a], Liang Ma[a], Guosu Wang[a], David Coe[a], Riccardo Ferro[b], Marco Falasca[b,c], Christopher D. Buckley[d], Claudio Mauro[a], and Federica M. Marelli-Berg[a,1]

[a]William Harvey Research Institute, Barts and The London School of Medicine and Dentistry, Queen Mary University of London, London EC1M 6BQ, United Kingdom; [b]Blizard Institute, Barts and The London School of Medicine and Dentistry, Queen Mary University of London, London EC1M 6BQ, United Kingdom; [c]Metabolic Signalling Group, School of Biomedical Sciences, Curtin Health Innovation Research Institute Biosciences, Curtin University, Perth, Western Australia 6102, Australia; and [d]Medical Research Centre Centre for Immune Regulation, University of Birmingham, Birmingham B15 2TT, United Kingdom

Constitutive resistance to cell death induced by inflammatory stimuli activating the extrinsic pathway of apoptosis is a key feature of vascular endothelial cells (ECs). Although this property is central to the maintenance of the endothelial barrier during inflammation, the molecular mechanisms of EC protection from cell-extrinsic, proapoptotic stimuli have not been investigated. We show that the Ig-family member CD31, which is expressed by endothelial but not epithelial cells, is necessary to prevent EC death induced by TNF-α and cytotoxic T lymphocytes in vitro. Combined quantitative RT-PCR array and biochemical analysis show that, upon the engagement of the TNF receptor with TNF-α on ECs, CD31 becomes activated and, in turn, counteracts the proapoptotic transcriptional program induced by TNF-α via activation of the Erk/Akt pathway. Specifically, Akt activation by CD31 signals prevents the localization of the forkhead transcription factor FoxO3 to the nucleus, thus inhibiting transcription of the proapoptotic genes CD95/Fas and caspase 7 and de-repressing the expression of the antiapoptotic gene cFlar. Both CD31 intracellular immunoreceptor tyrosine-based inhibition motifs are required for its prosurvival function. In vivo, CD31 gene transfer is sufficient to recapitulate the cytoprotective mechanisms in CD31⁻ pancreatic β cells, which become resistant to immune-mediated rejection when grafted in fully allogeneic recipients.

endothelium | immunology | inflammation | lymphocytes | transplantation

Maintenance of vascular integrity during inflammation is a major challenge in the cooperation between the immune and the vascular systems.

During acute inflammation, for example in solid organ transplantation, endothelial cells (ECs) can themselves become targets of innate and adaptive cytotoxic mechanisms, such as cytokines including TNF-α, and cytotoxic T lymphocytes (CTLs). However, with the exception of preformed antibody-triggered, complement-mediated responses in hyperacute responses, damage of the endothelium is relatively limited compared with that of other epithelial components, and the vasculopathy occurring during chronic rejection features abnormal perivascular responses leading to endothelial dysfunction rather than direct loss of ECs (1). How vascular integrity is maintained during inflammation has been the subject of intense investigation (2–4).

Two major apoptosis pathways, namely the intrinsic and extrinsic pathways, exist in mammalian cells (5). The first occurs under conditions of cellular stress (oxidative injury, irradiation, exposure to cytotoxic agents) via signals originating from the mitochondria. The second is activated when TNF-family proteins such as TNF-α and Fas ligand bind to TNF-family death receptors (DRs) on the cell surface or during T-cell–mediated cytolysis.

Although ECs express DRs on their surface, TNF-α and Fas ligand do not activate the extrinsic pathway of apoptosis in ECs efficiently (6). The molecular mechanisms underlying this effect remain elusive. Inhibition of the NFκB-dependent A1 or Bcl-x$_L$ prosurvival genes does not sensitize ECs to TNF-α–induced apoptosis, indicating that NFκB activation is not required for EC protection (7). In contrast, EC survival upon exposure to TNF-α or Fas ligand correlated with PI3K/Akt activation in a number of studies (8, 9). Human EC resistance to TNF-α– and LPS-induced apoptosis is dependent on new protein or mRNA synthesis, suggesting that an inducible or constitutively expressed endothelial protein is responsible for protection (10).

CD31, or platelet endothelial cell adhesion molecule-1, is a member of the Ig gene superfamily expressed at high density at the lateral borders of ECs and at a lower density on the surface of hematopoietic cells (11). By establishing homophilic interactions between endothelium- and leukocyte-expressed CD31, this molecule has been shown to be involved in leukocyte transendothelial migration in vitro and in vivo (11). CD31 signaling is mediated mainly by two immunoreceptor tyrosine inhibitory motifs (ITIMs) in its cytoplasmic tail (12). These ITIMs are phosphorylated upon CD31 engagement and subsequently serve as docking sites for protein-tyrosine phosphatases including the Src homology 2 domain-containing protein, SHP-2 (13).

CD31-deficient mice exhibit a very mild phenotype in steady-state conditions (14). However, these animals display exaggerated disease severity in inducible experimental models of T-cell–mediated inflammation, including experimental autoimmune encephalomyelitis (15), collagen-induced arthritis (16), atherosclerosis (17),

Significance

Maintenance of vascular integrity during effector immune responses occurring in tissues is a prerequisite of a healthy immune response. The mechanism whereby the vascular endothelium remains undamaged while interacting with effector immune cells migrating to the site of inflammation is largely unknown. This study shows that signals mediated by CD31, a *trans*-homophilic receptor expressed at high levels by the endothelium, are both necessary and sufficient to prevent inflammation-induced endothelial cell death and confer immune privilege to the vascular endothelium. We also provide proof of principle that this property can be harnessed therapeutically in pancreatic β-cell transplantation, whereby CD31 gene transfer alone endows allogeneic targets with indefinite resistance to immune attack in vivo.

and endotoxemia (18, 19), suggesting that CD31 signals play a protective role under conditions of immunological stress.

The involvement of CD31 signaling in EC protection from the intrinsic pathway of apoptosis, mostly in the context of exposure to toxic drugs, has been described previously (20, 21).

In contrast, despite the large body of evidence pointing to an endothelial-specific antiapoptotic pathway operational during immune-mediated cell death (18, 19), a potential role for CD31 in protecting ECs from inflammatory insults inducing the extrinsic pathway of apoptosis has not been investigated.

Results

CD31 Interactions Are Required for EC Protection from TNF-α– and CTL-Induced Cell Death. To investigate a potential role for CD31 in protecting ECs from the extrinsic pathway of apoptosis, we first compared the susceptibility of WT or CD31-deficient murine primary microvascular ECs to apoptosis induced by canonical cell-extrinsic apoptosis-inducing stimuli such as TNF-α and antigen-specific CTLs or necrosis induced by the complement.

As shown in Fig. 1 *A* and *B*, CD31-KO ECs exposed to TNF-α underwent a significantly higher rate of apoptosis than WT ECs.

Importantly, antibody blockade of CD31 activation (Fig. S1) increased the rate of TNF-α–induced apoptosis in subconfluent ECs (Fig. 1*C*), confirming that CD31 homophilic interactions between ECs are necessary to confer resistance to TNF-α–induced apoptosis.

We subsequently assessed the protective effect of CD31 expression by the endothelium from T-cell–mediated cytotoxicity. Lymphocyte-mediated cytotoxicity can be induced both by caspase-dependent apoptosis and by osmotic imbalance mediated by perforin leading to necrosis (22). EC death induced by CTLs therefore was measured by both TUNEL assay (selectively measuring apoptosis) and by Trypan Blue (TpB) exclusion (measuring overall cytolysis) in the same coculture. As shown in Fig. 1 *D* and *E*, HY-specific CTL-mediated killing was significantly increased in CD31-deficient male-derived ECs, indicating that CD31 expression can protect ECs from CTL-mediated cytolysis, in line with our previous observations with CD31-expressing antigen-presenting cells (23). In addition, overall cell death, as measured by TpB exclusion, was not quantitatively different from apoptosis, as measured by TUNEL, suggesting that the latter mechanism is dominant in CTL-mediated killing of ECs.

To establish whether CD31-mediated cytoprotection extended to mechanisms of cell death other than apoptosis, a comparison experiment was conducted on confluent murine ECs challenged with xenogeneic human serum as a source of complement-fixing antibodies (xenospecific IgM) and complement for 6 h. Because complement-induced cytolysis is largely independent of caspase activation, EC survival was assessed by TpB exclusion analysis, revealing similar levels of cell death in WT and CD31-KO ECs (Fig. 1*F*).

CD31 Is Required for the Activation of Erk/Akt Pathways Involved in EC Cytoprotection from Extrinsic Apoptosis. To investigate the molecular pathways involved in CD31-mediated EC survival upon extrinsic proapoptotic stimuli, we assessed whether CD31 is induced to signal upon TNF receptor (TNFR) engagement. EC exposure to TNF-α promoted an increase in CD31 phosphorylation and recruitment of the SHP-2 phosphatase to CD31-containing complexes, indicating that TNFR signaling activates CD31 (Fig. 2*A*).

We recently have shown that in T cells CD31-mediated protection from activation-induced cell death, which is largely Fas-dependent, is associated with Erk 1 and 2 but not NFκB activation (23). We therefore sought to assess whether the Erk/Akt pathway was induced in our system. We found low constitutive levels of Erk activation in WT and CD31-deficient ECs; these levels increased significantly in WT but not in CD31-deficient endothelium upon TNF-α stimulation (Fig. 2 *B* and *C*), suggesting that in ECs CD31 engagement is required for Erk activation downstream of TNFR signaling. Akt activation was induced following exposure of ECs to TNF-α in WT but not CD31-KO endothelium (Fig. 2 *B* and *D*). The key role of these mediators in protecting ECs from cell-extrinsic apoptosis was confirmed by experiments in which ECs were incubated with TNF-α following preincubation with selective Akt and ERK inhibitors; this incubation led to significantly increased apoptosis (Fig. 2*E*). Finally, Akt activation was reduced by blockade of CD31 antibody in WT ECs (Fig. 2*F*).

CD31 Promotes a Prosurvival Transcriptional Program Downstream of TNF-α Signals in ECs. Programmed cell death has been shown to be regulated by a coordinated transcriptional program in which the quantitative balance of pro- and antiapoptotic gene transcription can determine the ultimate outcome of inflammatory stimuli (5).
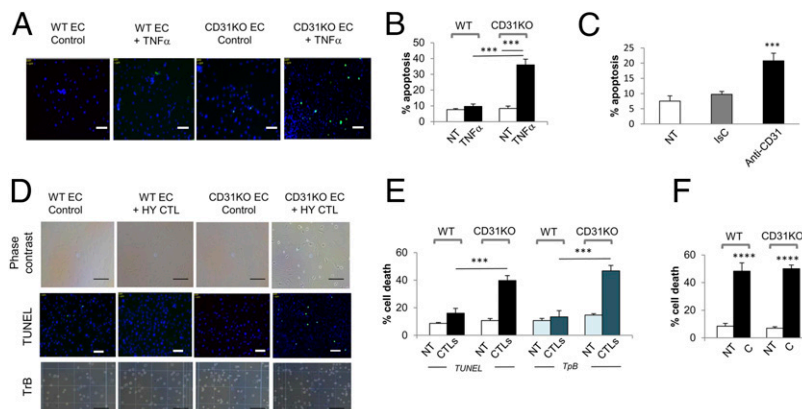

Fig. 1. CD31 protects from extrinsic apoptosis. (*A* and *B*) WT and CD31-KO ECs were exposed to TNF-α (50 ng/mL) for 6 h, and apoptosis was measured by TUNEL assay. (*C*) Alternatively, WT ECs were pretreated with either a blocking anti-CD31 or an isotype control antibody before exposure to TNF-α. (*D* and *E*) Male-derived murine ECs (pretreated with IFN-γ for 48 h to up-regulate MHC molecule expression) were incubated for 6 h with HY-specific CTLs (EC:CTL ratio 1:5), which were removed at the end of the incubation by gentle washing with warm PBS. EC death was measured by TUNEL assay and TpB exclusion assay. (*F*) ECs also were cultured in 10% (vol/vol) human serum as a source of antibody and complement, and cell death was measured by TpB exclusion assay. Representative images are shown in *A* and *D*. (Scale bars: 100 μm.) The mean percentages of apoptotic (*B*, *C*, and *E*) and necrotic (*F*) cells in three independent experiments (±SD) are shown. ***P < 0.001, ****P < 0.0001. NT, not treated.
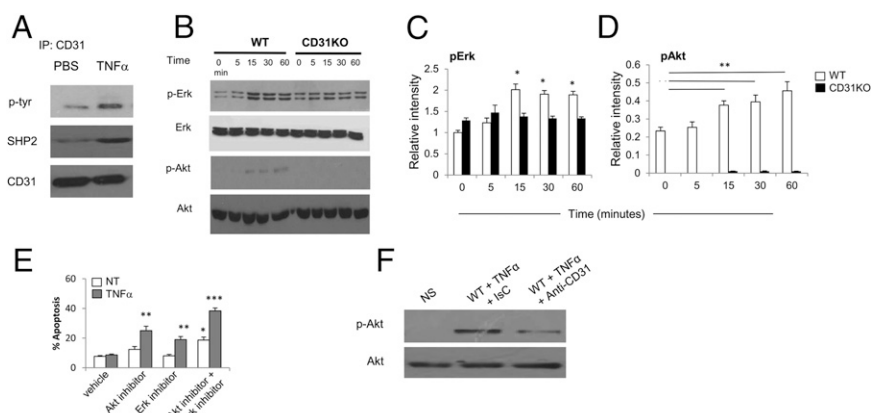
Fig. 2. Antiapoptotic pathways activated by CD31 in ECs. (*A*) Immunoprecipitation of CD31 molecules from ECs exposed to TNF-α for 20 min followed by immunoblotting with an anti-phosphotyrosine antibody and an anti-SHP2 antibody. (*B–D*) Erk (*B* and *C*) and Akt (*B* and *D*) activation in WT and CD31-KO ECs exposed to TNF-α; time points are indicated. (*E*) WT ECs were treated with an Akt inhibitor (3 μM) or with a MEK 1/2 inhibitor (10 μM) for 4 h at 37 °C before incubation with TNF-α. EC apoptosis was measured after 6 h by TUNEL assay. (*F*) Akt activation in WT ECs pretreated with a blocking anti-CD31 or an isotype control antibody and exposed to TNF-α for 30 min. In *C–E* the mean percentage of apoptotic cells in three independent experiments (±SD) is shown. *P < 0.05, **P < 0.01, ***P < 0.001.

To identify downstream mediators of the CD31 survival activity, we profiled the expression of apoptosis-related genes by WT and CD31-deficient ECs following exposure to TNF-α by using the RT2 profiler apoptosis array as described in *Methods*. The mRNA expression levels were normalized to untreated control cells.

Among the 84 genes analyzed, 19 were differentially regulated in either WT or CD31-KO ECs upon TNF-α stimulation (three uniquely in WT ECs, six uniquely in CD31-KO ECs, and 10 in both WT and CD31-KO ECs), but no significant differences in gene expression were observed when comparing resting WT (Dataset S1) and CD31-KO (Dataset S2) ECs (Fig. S2).

Based on pairwise comparisons of TNF-α–treated WT and CD31-KO ECs, the TNF-family DR CD95/Fas, the executioner Caspase family member caspase 7, and the antiapoptotic gene cFlar [CASP8 and Fas-associated protein with death domain (FADD)-like apoptosis regulator, also designated as cFLIP (Flice-like inhibitory protein)], were identified as genes that are transcriptionally repressed (Fas, caspase 7) or are transcribed de novo (cFlar) in WT but not in CD31-KO ECs in response to TNF-α.

The differential regulation of Fas and caspase 7 at the mRNA level was confirmed further by quantitative real-time PCR (qRT-PCR) Fig. 3 *A* and *D*) and at the protein and functional levels (Fig. 3 *B*, *C*, and *E*) by measuring Fas expression and caspase 7 activity by TNF-α–stimulated WT and CD31-deficient ECs via the use of flow cytometry and the Caspase 3/7 Assay. Because caspase 3 and 7 are shared by the intrinsic and extrinsic apoptosis pathways (5), inhibition of the latter by CD31 signals was confirmed by measuring caspase 8 activity (Fig. 3*F*).

We also compared the expression of programmed death ligand 1 (PDL-1), a negative costimulator of T cells not included in the RT2 profiler that is known to be expressed by the endothelium (4), and observed no differences between WT and CD31-deficient ECs (Fig. S3*A*).

We further observed that ECs express the serine protease inhibitor 6 (serpin B9/Spi6), known to provide protection from granzyme-induced cytotoxicity (22), and that Spi6 transcription was induced by exposure to TNF-α; however this transcription occurred independently of CD31 expression (Fig. S3*B*). Finally, we did not observe significant differences in reactive oxygen species (ROS) production by TNF-α–stimulated WT and CD31-deficient ECs (Fig. S3*C*), suggesting that CD31-mediated protection does not depend on the induction of antioxidant activity.
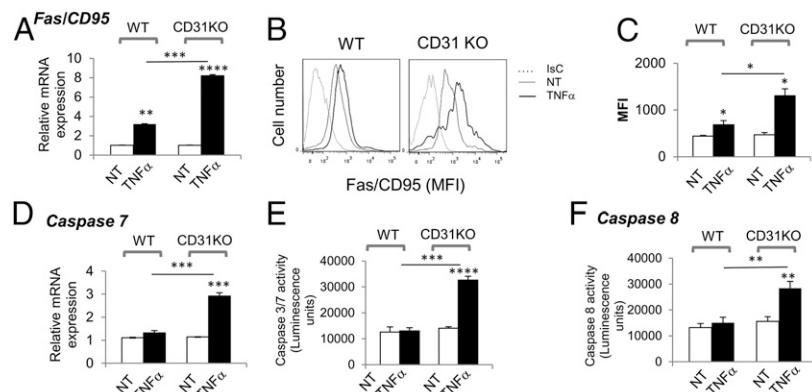

Fig. 3. CD31 modulates the proapoptotic transcriptional program downstream of DR signaling. (*A–C*) Expression of Fas mRNA and surface receptor by WT and CD31-KO ECs either untreated or exposed to TNF-α for 6 h as quantified by qRT-PCR (*A*) and flow cytometry (*B* and *C*). (*D–F*) Expression of caspase 7 mRNA and caspase 3/7 and caspase 8 activity by WT and CD31-KO ECs, either untreated or exposed to TNF-α as measured by qRT-PCR (*D*), ApoTox-Glo Triplex Caspase 3/7 (*E*), or Caspase 8 Reagent (*F*). In *A* and *C–F* cumulative data from three independent experiments (±SD) are shown. *P < 0.05, **P < 0.01, ***P < 0.001, ****P < 0.0001. MFI, mean fluorescence intensity.

cFlar is an antiapoptotic protein with significant homology to caspase 8 (24). By competitively binding to FADD and blocking the assembly of a functional death-inducing signaling complex (DISC), cFlar inhibits the activation of upstream initiator caspases, including caspase 8 (25). cFlar previously has been shown to be induced downstream of Akt and to be required for EC protection from LPS-induced apoptosis (10) as well as Fas-induced cell death (7). We therefore further investigated the involvement of this gene in the cytoprotective effect of CD31. qRT-PCR and immunoblotting experiments confirmed the lack of cFlar gene transcription and protein synthesis in CD31-KO ECs upon TNF-α stimulus (Fig. 4 A and B). cFlar knockdown by shRNA in WT ECs (Fig. 4 C and D) enhanced their sensitivity to TNF-α–induced apoptosis, and this enhanced sensitivity could not be rescued by CD31 antibody stimulation (Fig. 4E) (23).

Importantly, inhibition of Akt and Erk activation prevented cFlar expression by WT ECs exposed to TNF-α (Fig. 4F), suggesting that these pathways, which require CD31 expression for activation downstream of TNFR signaling (Fig. 2 B–F), directly mediate the induction of cFlar transcription.

We next asked how Akt induces cFlar expression downstream of CD31 signals. Akt activation is known to be antiapoptotic by multiple mechanisms. One of the best described is the phosphorylation of forkhead box O (FoxO) transcription factors, driving these proteins from the nucleus, where they induce the transcription of proapoptotic molecules and inhibit transcription of antiapoptotic ones (26). Of relevance here, FoxO proteins are known to inhibit cFlar transcription (27, 28). We therefore analyzed the distribution FoxO3 in WT and CD31-deficient ECs following exposure to TNF-α. As shown in Fig. 4 G and H, FoxO3 proteins were prevented from localizing in the nucleus in WT but not CD31-KO ECs upon TNF-α stimulation. Thus it is likely that CD31 signals block TNF-α–induced proapoptotic gene reprogramming by preventing nuclear localization of FoxO3 protein via activation of Akt.

Both Intracellular ITIMs Are Required for CD31 Antiapoptotic Activity.
Both ITIM-mediated signals and homophilic binding have been shown previously to be required for efficient CD31 protection from the intrinsic apoptotic pathway (20). To investigate whether these signaling domains also are required for CD31-mediated inhibition of the extrinsic pathway, we generated two CD31 gene constructs with mutations leading to the loss-of-function amino acid substitutions Y663F and Y686F in the ITIMs, which were lentivirally transduced into CD31-KO ECs (CD31[Y663F] and CD31[Y686F] ECs). As shown in Fig. 5, both CD31[Y663F] and CD31[Y686F] mutant receptors fail to protect ECs (Fig. 5A) from TN-Fα– and CTL-mediated apoptosis (Fig. 5 B–D) and exhibited impaired Erk and Akt activation compared with CD31 WT ECs (Fig. 5 E–G). Furthermore neither mutant was able to suppress TNF-α–induced expression of CD95/Fas (Fig. 5 H and I) or the transcription and activity of caspase 7 and 8 (Fig. 5 J–L), or promote the expression of cFlar (Fig. 5M), and both failed to prevent the localization of FoxO protein to the nucleus upon exposure to TNF-α (Fig. 5 N and O).

As expected, expression of Spi6 was not affected in CD31[Y663F] and CD31[Y686F] ECs (Fig. S4). Overall these data suggest that both CD31 ITIMs are required for CD31-mediated EC cytoprotection.

CD31 Expression Confers Resistance to Cytolysis by Alloreactive T Cells and Promotes Graft Survival.
We next sought to establish whether CD31's antiapoptotic activity is both necessary and sufficient to maintain EC survival during activation of the extrinsic pathway of apoptosis in physiologic immune responses.

Rejection of HY-mismatched skin grafts is dependent on antigen presentation by the endothelium (29), and skin is a major target of graft-versus-host disease (GVHD), which is affected by CD31 polymorphism in humans (30). Therefore, we first compared rejection of male-derived WT and CD31-KO skin grafts by syngeneic female recipients. Analysis of the vascular endothelium at day 7 after transplantation revealed the maintenance of the
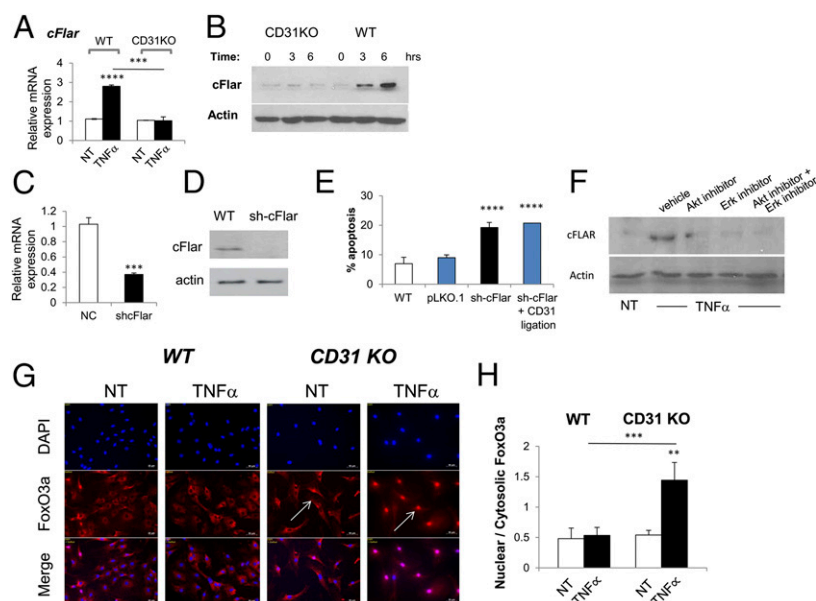

Fig. 4. The antiapoptotic gene cFlar is instrumental to CD31-mediated cytoprotection. mRNA was isolated from CD31-KO or WT ECs either untreated or stimulated with TNF-α (50 ng/mL) for 6 h. (A and B) cFlar mRNA quantification (A) and protein expression (B) by WT and CD31-KO ECs after incubation with TNF-α. (C and D) cFlar expression by ECs following shRNA knockdown was evaluated by qRT-PCR (C) and immunoblotting (D). (E) Apoptosis of ECs exposed to TNF-α following cFlar knockdown measured by TUNEL assay. In some cFlar-silenced cells, CD31 was stimulated by antibody ligation. pLKO.1 indicates cells transduced with the empty vector backbone. (F) WT ECs were treated with an Akt inhibitor (3 μM) or a MEK1/2 inhibitor (10 μM) before incubation with TNF-α. Expression of cFlar was measured after 6 h. (G and H) EC cultures were fixed, and FoxO3a intracellular localization was assessed by immunofluorescence staining. Nuclei were stained with DAPI. Representative images are shown in G. (Scale bars: 50 μm.) H shows the quantification of immunofluorescence staining patterns for endogenous FOXO3 (n = 100 cells per experiment). The data shown in A, C, E, and H are the mean value (±SD) of three independent experiments. **P < 0.01, ***P < 0.001, ****P < 0.0001.
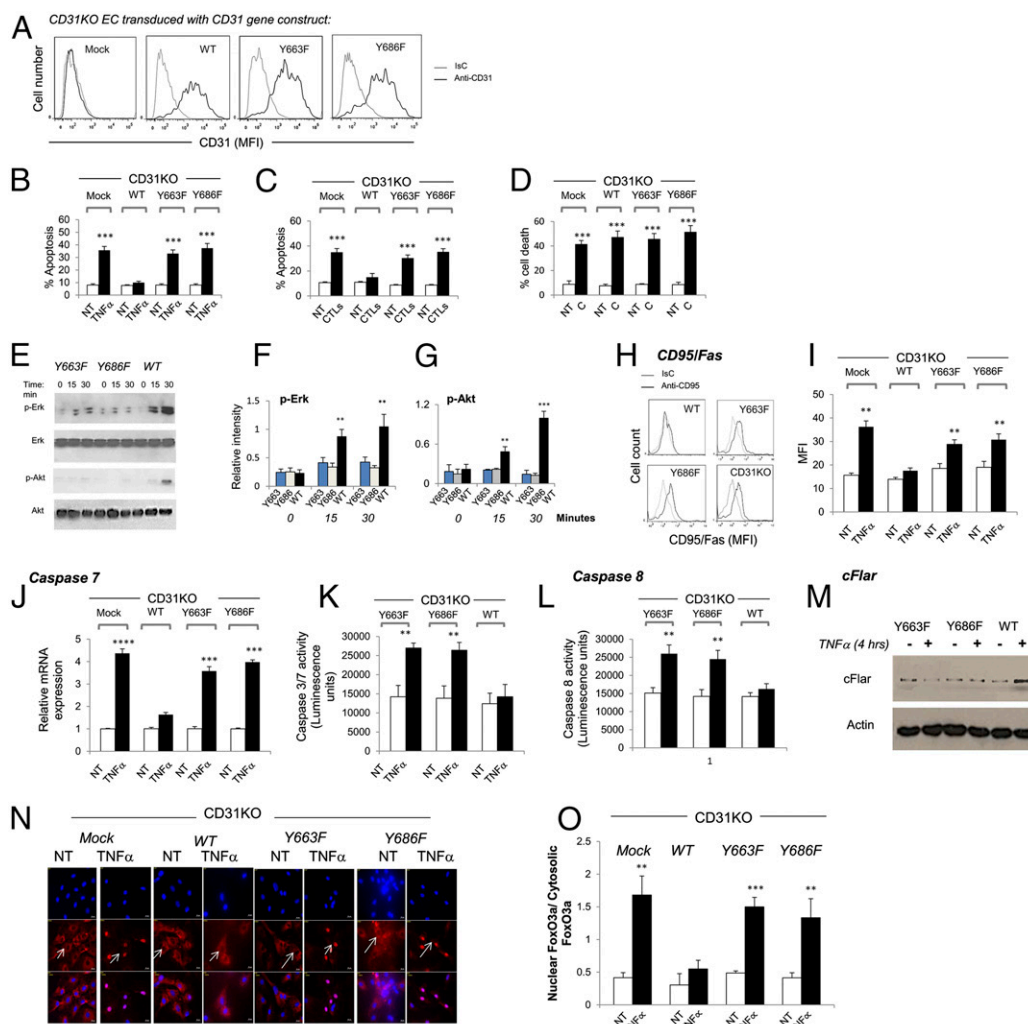
Fig. 5. Both CD31 ITIMs are required for its prosurvival activity. CD31 gene constructs with mutations leading to the loss-of-function amino acid substitutions Y663F and Y686F in the ITIMs were generated and expressed by lentiviral transduction into CD31-KO ECs (CD31^{Y663F} and CD31^{Y686F}). As a control, CD31-KO ECs were transduced with a WT CD31 gene construct or an empty plasmid (mock). (*A*) Surface expression of CD31^{Y663F} and CD31^{Y686F} molecules following transduction of CD31-KO ECs. As a control, WT CD31 and empty plasmid (mock) constructs were used. (*B* and *C*) Apoptosis of mock-, WT-, CD31^{Y663F}-, and CD31^{Y686F}-transduced CD31-KO ECs either exposed to TNF-α for 6 h or cocultured with antigen-specific CTLs for 6 h, as measured by TUNEL assay. (*D*) Complement-mediated lysis of the indicated EC populations. (*E–G*) Erk and Akt activation in ECs transduced with the indicated constructs following exposure to TNF-α. (*H–M*) CD95/Fas surface expression (*H* and *I*), caspase 7 expression and activity (*J* and *K*), caspase 8 activity (*L*), and cFlar protein expression (*M*) in the indicated EC populations, either untreated or exposed to TNF-α for 6 h. In *B–D*, *F*, *G*, and *I–L* the mean value of data measured in three independent experiments (±SD) is shown. **$P < 0.01$, ***$P < 0.001$, ****$P < 0.0001$. (*N* and *O*) Mock-, WT-, CD31^{Y663F}- and CD31^{Y686F}-transduced ECs were fixed, and FoxO3a intracellular localization was assessed by immunofluorescence staining. (*N*) Nuclei were stained with DAPI, and representative images were taken by deconvolution wide-field immunofluorescence microscopy. (Scale bars: 50 μm.) (*O*) Quantification of immunofluorescence staining patterns for endogenous FoxO3 (*n* = 100 cells per experiment). Data represent the mean value (±SD) of three independent experiments. **$P < 0.01$, ***$P < 0.001$, ****$P < 0.0001$.

donor vasculature within the graft (Fig. S5 *A–D*) and the establishment of direct anastomosis of the donor's and recipient's vasculature (Fig. S5*E*), indicating that this model is suitable for assessing vascular rejection. As shown in Fig. 6*A*, the survival of CD31-deficient skin grafts was reduced significantly compared with that of WT skin. As expected, both CD31-KO and WT female-derived control grafts survived indefinitely. Male-derived WT skin grafts excised at day 14 after transplantation displayed relatively moderate mononuclear cell infiltration with preservation of hair follicles and vessels in the dermis on histological examination (Fig. 6 *B* and *C*). CD31-deficient male-derived skin grafts displayed thinning of the epidermis accompanied by extensive necrosis of dermis tissue and hair follicles and, importantly, EC damage and loss in small vessels (Fig. 6 *D* and *E*) despite similar mononuclear cell infiltrates. All these features are indicative of overwhelming

vascular damage. However, to rule out the possibility that CD31-deficient dendritic cells of graft origin might have enhanced the proliferation of HY-specific CTLs, we quantified HY-specific CD8$^+$ T cells in the graft-draining lymph nodes 7 d after transplantation (i.e., at the peak of T-cell expansion) by Uty tetramer staining. We did not detect any differences in the number of HY-specific T cells rejecting WT or CD31-KO male skin grafts (Fig. 6 *F* and *G*).

To confirm the nonredundant protective role of CD31 in allograft rejection, we tested whether transfer of CD31 expression would endow cells that do not physiologically express this molecule with resistance to extrinsic apoptosis. CD31$^-$, H2^b-expressing MIN6 (28) pancreatic β cells were transduced with the WT CD31 gene or were mock-transduced with the empty vector (Fig. 7*A*). The efficiency of gene transfer (shown in Fig. 7*A*) did not affect insulin production in response to glucose stimulation in nontreated
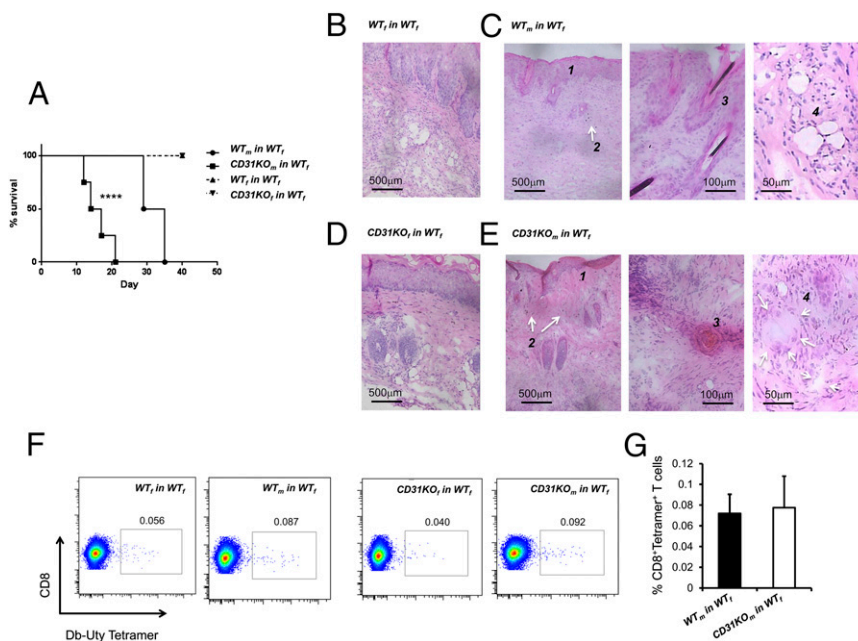
Fig. 6. Enhanced rejection of CD31-deficient skin grafts. WT female mice received either a WT or CD31-KO male-derived skin graft. As a control, female WT and CD31-KO female-derived skin was used. (*A*) Graft survival (*n* = 6). ****P < 0.0001. (*B–D*) In some recipients, WT or CD31-KO grafts were harvested 14 d after transplantation. Representative tissue sections of grafts from female WT (*B*) and CD31-KO (*D*) controls and male WT (*C*) and CD31-KO (*E*) mice stained with H&E. 1, epidermis; 2, mononuclear inflammatory cells; 3, hair follicles; 4, dermis vessels. (*F* and *G*) Allograft-draining lymph nodes were harvested 7 d posttransplantation, and the presence of HY-specific CD8 T cells was evaluated by tetramer staining. (*F*) Representative dot-plots. (*G*) The mean percentage of CD8⁺ tetramer⁺ T cells from six animals.

cells (Fig. 7*B*). Transduction of the CD31 gene in MIN6 cells fully recapitulated the cytoprotective effects observed in ECs, including maintenance of insulin production (Fig. 7*B*) and resistance to TNF-α–induced cell death (Fig. 7 *C* and *D*) and CTL-mediated cytolysis (Fig. 7 *E* and *F*). Interestingly, the protective effect of CD31 on CTL-mediated lysis of pancreatic β cells was not as complete in MIN6 cells as in ECs (Fig. 1 *D* and *E*). MIN6 cell killing was prevented completely only by the inhibition of both DR signaling and lytic granule release (Fig. 7*G*), indicating that perforin-induced osmotic lysis is only partially inhibited by CD31 signals. FoxO3, which has been implicated in osmotic lysis (31), localized to the nucleus only in mock-transduced but not in CD31-expressing MIN6 cells after incubation with CTLs (Fig. 7*H*).

Similar to our observations in ECs (Fig. 1*C*), antibody blockade of CD31 in transduced MIN6 cells significantly increased their susceptibility to CTL-induced death (as measured by TpB) to the levels observed when mock-transduced cells were used as targets (Fig. 7*I*).

The acquired resistance of MIN6 cells to TNF-α and CTL-induced death was associated with activation of the Erk/Akt pathway (Fig. 8*A*), down-regulation of Fas (Fig. 8*B*), caspase 7 expression and activity (Fig. 8 *C* and *D*), caspase 8 activity (Fig. 8*E*), up-regulation of cFlar expression (Fig. 8*F*), and inhibition of FoxO3 nuclear localization (Fig. 8*G*).

Like ECs, MIN6 cells were found to express the Spi6 gene and up-regulate its transcription upon TNF-α stimulation (Fig. S6). However, transduction of CD31 did not modify its expression and indeed resulted in a lower level of up-regulation following exposure to TNF-α, suggesting that this molecule is not implicated in the acquired resistance to perforin-mediated apoptosis by CD31-expressing MIN6 cells.

Collectively, these data suggest that expression of CD31 confers cytoprotection to MIN6 cells by mechanisms very similar to those observed in ECs.

To establish whether CD31 expression is sufficient to prevent the induction of cell-extrinsic apoptosis, as in CTL-mediated allograft rejection, in physiologic settings, we chose to assess rejection of CD31-expressing pancreatic β cells grafted in a fully allogeneic recipient.

Mock- or CD31-transduced MIN6 cells were grafted under the renal capsule of BALB/c mice that had been rendered diabetic by injection of streptozotocin (STZ) 3 wk earlier. As a control, WT MIN6 cells were grafted in syngeneic C57BL/6 diabetic mice, leading to complete normalization of glycemia (Fig. 9*A*). As shown in Fig. 9*B*, diabetes persisted in recipients of WT MIN6 cells, indicating transplant rejection. In contrast, in recipients of CD31-expressing MIN6 cells glycemia returned to normal for the duration of the experiment. Healthy CD31-expressing MIN6 islets were detected in the kidney of these recipients, suggesting that these cells had become resistant to rejection (Fig. 9 *C* and *D*).

An analysis of anti–H-2D alloresponses revealed that these responses were conserved both in animals that received WT and those that received CD31-expressing MIN6 cells (Fig. 9*E*), suggesting that CD31 transduction led to the induction of immune privilege rather than tolerance.

Discussion

We report here that the Ig-family receptor CD31, which is selectively expressed by ECs at high density, becomes activated upon the delivery of proapoptotic immune stimuli and is both necessary and sufficient to prevent EC death as a consequence of these signals. Importantly, we show that the apoptotic stimuli themselves induce CD31 activation, which in turn counteracts the proapoptotic gene reprogramming initiated by such stimuli. Because EC cultures are nonconfluent, it is likely that CD31 signaling triggered by TNF-α is initiated by *cis* interactions of CD31 molecules. This mechanism also is supported by the observation that the anti-CD31 antibody, which has been shown to prevent *cis* interactions by CD31 (32), inhibited CD31-mediated prosurvival activity induced in response to TNF-α. Activation of CD31 signaling by CTLs is likely to be induced by distinct mechanisms: first, CTLs' interaction with EC might lead to
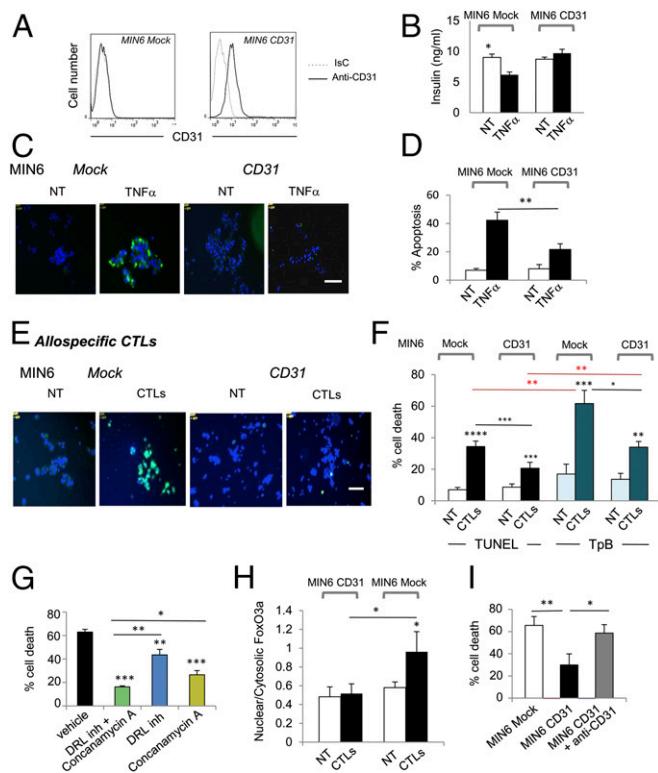
Fig. 7. CD31-transduced pancreatic β cells are protected from extrinsic apoptosis. (A) Surface expression of CD31 by mock- and CD31-transfected MIN6 cells. (B) Insulin secretion by untreated and TNF-α–exposed mock- and CD31-transfected starved MIN6 cells incubated in DMEM containing 2.8 mM glucose for 30 min at 37 °C, measured 1 h after reconstitution with 25 mM glucose. (C–F) Cell death of mock- and CD31-transfected MIN6 cells either exposed to 50 ng/mL TNF-α for 6 h (C and D) or cocultured with allospecific CTLs for 6 h (E and F) as measured by TUNEL and TpB assays. Representative images are shown in C and E. (Scale bars: 100 μm.) (G) Apoptosis of mock- and CD31-transfected MIN6 cells cultured with allospecific CTLs for 6 h and pretreated with a DR ligand (DRL) inhibitor (5 μM) and/or concanamycin A (5 μg/mL) for 1 h. (H) FoxO3a intracellular localization in MIN6 cells was assessed by immunofluorescence staining following coculture with CTLs (MIN6:CTL ratio 1:5) for 6 h. Quantification of immunofluorescence staining patterns for endogenous FOXO3 is shown (n = 100 cells per experiment). (I) Apoptosis of CD31-transfected MIN6 cells cultured with CTLs for 6 h following treatment with a blocking anti-CD31 antibody or isotype control. Mock-transduced cells are included for comparison. Data in B, D, and F–I are the mean percentage (±SD) of apoptotic cells measured in three independent experiments. *P < 0.05, **P < 0.01, ***P < 0.001, ****P < 0.0001.

trans-CD31 ligation (23). Alternatively, CD31 might be activated indirectly by MHC ligation by the T-cell receptor (33).

Activated inflammatory cells, including the endothelium, undergo active shedding of the extracellular domain of the CD31 molecule (34, 35); this shedding could contribute to the loss of cell–cell adhesion (34) and to the rise in circulating soluble (s)CD31 during inflammatory diseases (35). Although a potential physiologic role of sCD31 serum levels in vivo remains to be determined, the membrane-anchored truncated protein remains capable of signaling (35); hence, the loss of the CD31 extracellular domain should not affect its ability to interfere with apoptosis.

Rather than interfering with proapoptotic signaling pathways directly, CD31 signals prevent ad hoc proapoptotic genetic reprogramming by redirecting the transcription factor FoxO3 to the cytoplasm via Akt-mediated phosphorylation (Fig. S7). This is a previously unknown pathway for the acquisition of immune privilege.

Tissue immune privilege, originally thought a consequence of the inability of immune cells to access target tissue, is currently

viewed as the ability of the tissue itself to downmodulate T-cell effector function during cognate recognition of self- and allo-antigens (36). For example, expression of Fas ligand by cells in the anterior chamber of the eye and by the Sertoli cells in the testis preserves their integrity against immune attack by inducing death of CD95 (Fas)-expressing T lymphocytes (37, 38). Privileged tissues also feature other protective mechanisms, such as a tight endothelial barrier, down-regulation of MHC molecules, and production of anti-inflammatory cytokines such as TGF-β. The term "immune privilege" also implies that the protective mechanism(s) apply only to selective cellular components (36). A plethora of signals have been proposed to sustain EC survival in vivo, including adhesion to the basement membrane and to adjacent ECs, growth factors, and survival signals derived from pericytes (6). However, most of these signals selectively prevent mitochondrial apoptosis. In addition, a number of mechanisms have been identified that modulate EC activation or deliver inhibitory signals to cytotoxic T cells; for example, the Down syndrome critical region gene 1, which is induced by inflammatory mediators, reduces the expression of ICAM-1, VCAM, and E-selectin by ECs (2). ECs also can regulate CTL responses negatively by expressing coinhibitory receptors such as Herpes simplex entry mediator (3) and programmed cell death ligand-1 (4). However, these mechanisms also apply to cells of nonendothelial lineage, which nevertheless are susceptible to immune-mediated damage.

Our study indicates that CD31, which is expressed specifically at high levels by ECs, selectively endows the vascular endothelium with the ability to maintain vascular integrity actively during immune inflammation and as such behave like an immune-privileged tissue. Our observations further suggest that, in response to extrinsic apoptotic stimuli, CD31 engages a prosurvival pathway that is distinct from that induced by intrinsic stimuli (20), with
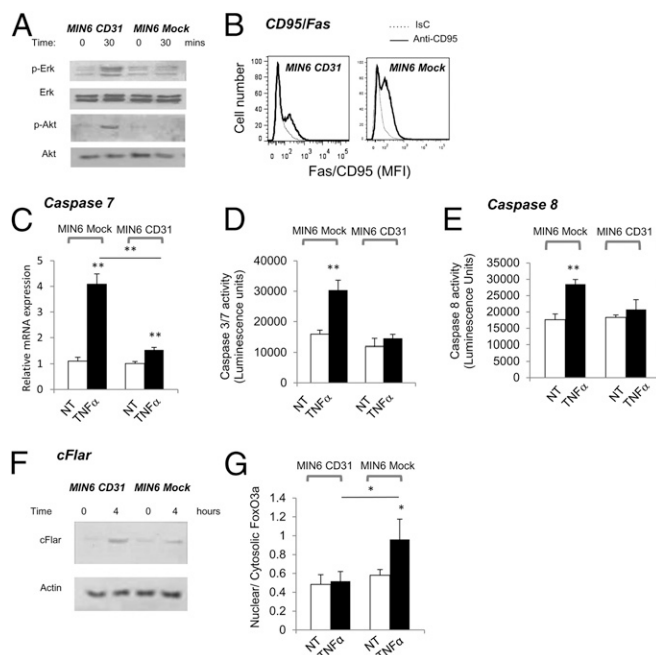

Fig. 8. Antiapoptotic pathways activated in CD31-transduced pancreatic β cells. (A–F) Erk and Akt activation (A), Fas surface expression (B), caspase 7 expression and activity (C and D), caspase 8 activity (E), and cFlar protein expression (F) by mock- and CD31-transfected MIN6 cells exposed to TNF-α for 6 h. (G) Nuclear localization of FoxO3 in MIN6 cells exposed to TNF-α for 6 h. Quantification of immunofluorescence staining patterns for endogenous FOXO3 is shown (n = 100 cells per experiment). Data in C–E and G are the mean value (±SD) of three independent experiments. **P < 0.01.
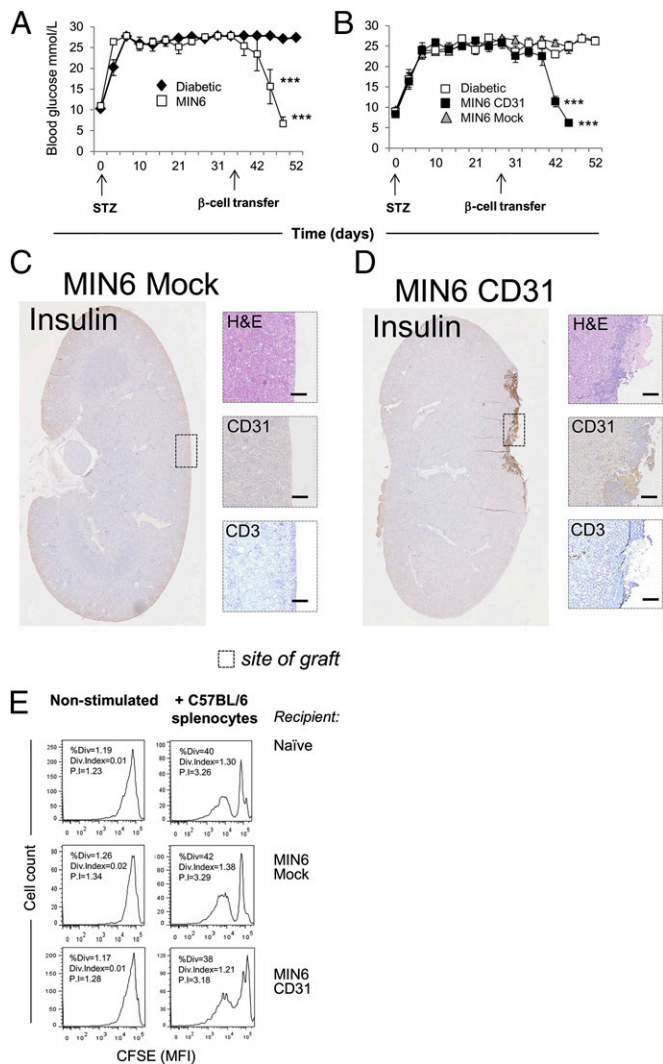
Fig. 9. CD31-expressing pancreatic β cells become resistant to T-cell–mediated allograft rejection. (*A* and *B*) The function of mock-transduced and CD31 MIN6 islets was evaluated by measuring blood glucose levels in grafted syngeneic (C57BL/6) (*A*) or allogeneic (Balb/C) (*B*) mice rendered diabetic by STZ injection. (*C* and *D, Left*) Representative images of a kidney that received either mock- or CD31-transduced MIN6 β cells and was stained to detect insulin production. (*Right*) Magnified sections of the grafts processed as indicated. (Scale bars: 100 μm.) (*E*) At the time mice were killed, T cells were isolated from the spleen and lymph nodes of recipients and labeled with carboxyfluorescein succinimidyl ester (CFSE). Cell division in response to an ex vivo rechallenge with C57BL/6 splenocytes by T cells from naive mice (recipients of mock-transduced or CD31 MIN6 cells) was measured by flow cytometry. Representative histograms show percent division, division indices, and proliferation indices as determined by FlowJo. **$P < 0.01$, ***$P < 0.001$.

the Akt/Erk pathway being dominant during extrinsically induced apoptosis.

Interestingly, cellular resistance to immune-mediated cell death correlates strictly with CD31 expression in some cells of hematopoietic origin. We previously have reported that CD31 reduces cytotoxic killing of antigen-presenting cells (23). Selective expression of CD31 by endothelium and dendritic cells may serve the purpose of preserving their integrity and function during immune inflammation; thus, the endothelium can mediate the development of inflammatory infiltrates without being damaged by migrating activated leukocytes, and antigen-presenting dendritic cells can serially activate multiple cognate T cells without themselves being

killed at the first encounter. Intriguingly, aberrant expression of CD31 has been described in some tumors and correlates with adverse prognosis (21), leading to the hypothesis that CD31 expression by nonendothelial tumors may facilitate metastasis via its ability to bind homophilically to endothelial CD31 and/or by conferring resistance to chemo- and radiotherapy (21). Based on our observations, prosurvival signals generated by CD31 interactions also might be harnessed by tumors to become resistant to immune attack.

In support of a physiologic role of CD31 in protecting the endothelium from immune-mediated damage, we show that loss of CD31 expression by skin allografts leads to accelerated rejection featuring extensive vascular damage and necrosis rather than overwhelming T-cell activation and inflammation. In line with our findings, enhanced endothelial loss was prominent during the rejection of CD31-deficient aortic transplants (17).

Finally, we show that CD31 gene transfer is sufficient to recapitulate the cytoprotective mechanisms in CD31⁻ pancreatic β cells, which become resistant to immune-mediated rejection when grafted in fully allogeneic recipients. This finding is an unexpected and previously unreported observation, with potential therapeutic impact.

The ability of CD31 expression to protect MIN6 cells from CTL-mediated killing appears to affect not only DR-induced apoptosis but also perforin-mediated lysis, which does not play a significant role in EC cytolysis. The molecular mechanism of this effect is unclear at present, and it does not involve induction of the Serpin inhibitor Spi6. Notably, IL-4–induced phosphorylation of another FoxO family member, FoxO1, has been shown to prevent EC cytolysis by up-regulating claudin-5 expression and junction tightness (31).

In addition to their relevance in basic vascular physiology, the findings described here might have a broader impact on vascular pathology. CD31 has been implicated in the development of atherosclerosis and its clinical complications (39, 40). A few studies have described a link between the development of human atherosclerosis and the presence of CD31 SNPs. Interestingly, a number of the CD31 SNPs that have been associated with atherosclerosis (41–44) are the same as those implicated in increased GVHD severity (45–49). The functional significance of these SNPs has yet to be explored, and their association with disease remains controversial (50). However, it is interesting that the SNP at position 670 is located in proximity to the cytoplasmic ITIMs, which, as we show, are key for CD31 signal transduction and prosurvival activity.

Methods

Mice. CD31-KO mice were generated as previously described (14), backcrossed on the C57BL/6 background, and bred in house. Age- and weight-matched WT C57BL/6 mice were purchased from Charles River. All mice in this study were used between the ages of 4 and 11 wk. All in vivo experiments were conducted under the Home Office regulation following approval by the Queen Mary University of London Ethics Committee.

Reagents and Antibodies. The reagents used in this study include recombinant murine TNF-α (PeproTech), AKT inhibitor (Akt Inhibitor X; Calbiochem), and ERK inhibitor (PD98059; Cell Signaling). The vacuolar type H⁺-ATPase inhibitor concanamycin A, which completely blocks perforin-based cytotoxic activity by T lymphocytes, was purchased from Santa Cruz Biotechnology. The DR inhibitor CAS 1049741-03-8 was purchased from Merck Millipore. The antibodies used in this study include anti–P-Akt (ser-473) (1:1,000), anti–Akt (1:1,000), anti–P-ERK1/2 (1:1,000), anti–ERK1/2 (1:1,000; Cell Signaling), anti–P-tyrosine (PY20; 1:500), anti-SHP2 (1:500; Abcam); anti–FLIP-L (1:500), and anti–α-actin (1:1,000; Santa Cruz Biotechnology). For staining of the endothelium in skin grafts and EC cultures, rat anti-mouse CD31 antibody (102501; BioLegend) and sheep anti-mouse von Willebrand factor (VWF) (ab11713; Abcam) and secondary antibodies Alexa Fluor 488 donkey anti-sheep IgG (H+L) (A-11015; Life Technologies) and Alexa Fluor 594 donkey anti-rat IgG (H+L) (A-21209; Life Technologies) were used. For flow cytometry staining rat anti-mouse CD31 antibody clone 390 (eBioscience) was used. The IgG2a, kappa, and Rat IgG2a K Isotype Control Purified (clone eBR2a) were purchased from eBioscience. As a blocking reagent (Fig. S1), rat

anti-mouse CD31 Antibody clone 390 (eBioscience) was used at a concentration of 10 μg/mL. To stimulate signaling, CD31 molecules were ligated with polyclonal rabbit anti-mouse CD31 (5 μg/mL) (ab28364; Abcam) plus goat–anti-rabbit Ig (2.5 μg/mL) (Thermo Scientific). For the detection of HY-specific T cells, phycoerythrin (PE)-conjugated D^b-Uty Tetramer (peptide WMHHNMDLI; Medical and Biological Laboratories Co. Ltd.) and FITC-conjugated rat anti-mouse CD8 (11-0081-85; eBioscience) were used.

Cell Cultures. Murine ECs were purified from WT and CD31$^{-/-}$ mouse lung tissue as described previously (51). ECs were serially subcultured at 37 °C with 5% CO_2 in DMEM supplemented with 2 mM glutamine, 100 μg/mL penicillin, 100 μg/mL streptomycin, 1 mM sodium pyruvate, 10 mM Hepes, 1% nonessential amino acids (all from Life Technologies), and 50 μM 2-mercaptoethanol (Sigma-Aldrich), with freshly added 20% (vol/vol) heat-inactivated FCS (Labtech International) and 75 μg/mL EC growth supplement (Sigma-Aldrich) in 2% (vol/vol) gelatin-coated (Sigma-Aldrich) tissue-culture flasks. At confluence, ECs were detached from the culture flasks using trypsin/EDTA (Life Technologies) and were passaged. In all experiments, ECs were used between passages 3 and 4.

CD8$^+$ HY (male)-specific H2-D^b–restricted CTLs were generated by stimulation of T cells isolated from the lymph nodes of C57BL/6 female mice with splenocytes isolated from syngeneic male mice and IL-2 (20 U/mL; Roche) for 10 d in RPMI medium 1640 supplemented with 10% (vol/vol) FCS (Labtech International), 2 mM glutamine, 50 μg /mL penicillin, 50 μg/mL streptomycin, and 50 μM 2-mercaptoethanol (all from Life Technologies). CD8$^+$ T cells were subsequently isolated by immunomagnetic negative selection (Miltenyi Biotech) before use.

In cytotoxicity assays T cells were incubated with IFN-γ–treated ECs derived from WT and CD31-deficient female mice (H-2^b background) pulsed with the HY-derived Uty peptide (52). As a control non–peptide-pulsed ECs were used.

MIN6 cells (SV40 T-transformed pancreatic β cells derived from NOD mice) were grown in DMEM culture medium containing 25 mM glucose (Life Technologies) supplemented with 15% (vol/vol) FBS, 2 mM glutamine, 100 μg/mL penicillin, and 100 μg/mL streptomycin.

Complement Lysis Assay. As a source of complement and complement-fixing xenoantibodies, human serum was obtained after sedimentation of blood of healthy donors (Queen Mary Ethics of Research Committee Ethical Approval QMERC2014/61). Sterile tubes without any anticoagulants were used to separate serum from the blood cells, and the tubes were left in a standing position for about 20–30 min before centrifugation at 1,500 × g at 20 °C for 10 min. Serum then was extracted and frozen at −80 °C. In cell lysis assays, the human serum was diluted 1:10 in RPMI medium and then was added to murine EC monolayers, which were incubated at 37 °C.

Gene-Expression Analysis by qRT-PCR. Total RNA was extracted with TRIzol (Life Technologies), purified using the PureLink RNA minikit (Life Technologies), and assessed for quality and quantity using absorption measurements. RNA with an RNA integrity number of ≥7.6 was used for analysis of apoptosis using pathway-focused RT-PCR array systems (RT2 Profiler PCR Array Mouse Apoptosis; Qiagen) and an Applied Biosystems 7500 Fast Real-Time PCR machine (Life Technologies). Ct values were gathered using 7500 Fast System SDS Software (Applied Biosystems). Comparative data analysis was performed via the ΔΔCt method using the PCR Array Data analysis web portal (www.sabiosciences.com/RTPCR.php) to determine relative expression differences between the comparison groups. Changes of mRNA abundances by twofold and higher with a *P* value <0.05 were considered significantly different between the comparison groups as shown. Confirmation studies and relative quantification of additional genes was performed using the QuantiFast SYBR Green RT-PCR Kit (Qiagen) with 100 ng RNA per reaction and following the manufacturer's protocol. Specific primers for qRT-PCR were designed with the help of online tools (Primer 3Plus) using at least one exon junction-binding site per primer pair. Sequences of the qRT-PCR primers are as follows:

CD95 (5′-ATGCTGGGCATCTGGACCCT-3′ and 5′-CAACATCAGATAAATTTA-TTGCCAC-3′);

cFlar (5′-GACCCTTGTGCTTCCCTA-3′ and 5′-GTTAATCACATGGAACAATT-TCC-3′);

Caspase 7 (5′-CTACCGCCGTGGGAACGATGGCAGA-3′ and 5′-CGAAGGCC-CATACCTGTCACTTTATC-3′);

Spi6 (5′-CAGAGTTGTTGTCAGGTGGC-3′ and 5′-CGACACATCATCTGCAC-TGG-3′);

GAPDH (5′-AGAACGGGAAGCTTGTCATCA-3′ and 5′-GACCTTGCCCACAGC-CTTG-3′).

The thermal cycling profile for amplification was 95 °C for 10 min, followed by 40 cycles of 95 °C for 15 s and 54 °C for 1 min. Amplification was 95 °C for 10 min, followed by 40 cycles of 95 °C for 15 s and 60 °C for 1 min. To ensure the amplification specificity, the melting curve program was set as follows: 95 °C for 15 s, 60 °C for 1 min, and 95 °C for 15 s, right after the PCR cycles.

FoxO3a Staining. EC cultures were fixed and stained with an anti–FKHRL-1 (EP1949Y) (1:50) (Abcam) and the secondary antibody Alexa-Fluor 555. FoxO3a patterns of intracellular localization were quantified using specifically designed software to run in the LabView version 7.1 (National Instruments) environment. This automatic cell-counting algorithm is based on a combination of background subtraction, multiple thresholding, and morphological processing approaches (53).

Caspase Activity Assays. For caspase 3/7 measurements, cells were seeded in 96-well plates and incubated with or without inflammatory stimulus. Then, Caspase-Glo 3/7 or Caspase 8 Reagent (Promega) was added according to the manufacturer's protocol. The samples were incubated for 15 min in the dark and then were analyzed. Luminescence intensity was measured with a fluorometric imaging plate reader (BioTek Instruments).

Lentivirus Preparation for Gene Silencing and Overexpression. Bacterial glycerol stocks containing shRNA plasmid clones targeting cFlar cloned in the pLKO.1 vector were purchased from Sigma. Lentivirus packaging and envelope vectors pMDLg/pRRE, pRSV-Rev, and pENV were purchased from Addgene. cDNA of murine CD31 fused in-frame with GFP at the C terminus was used as template to generate tyrosine-to-phenylalanine (Y-to-F) mutations at the amino acids residues 663 and 686 (Y663F or Y686F, respectively) using the QuikChange site-directed mutagenesis kit (Stratagene). WT, Y663F, and Y686F CD31 cDNAs were subcloned into the pWPT lentiviral expression vector at MluI and SalI restriction sites and were checked by sequencing. Lentivirus packaging and envelope vectors R8.91 and MD2G were purchased from Addgene. HEK293T cells were grown in 10 × 10 cm cell-culture dishes to 70% confluence and were transfected with the plasmids listed above using the calcium phosphate method. The supernatant was harvested 48 and 72 h after transfection and was concentrated 100-fold in an ultracentrifuge. Aliquots were stored at −80 °C.

Lentiviral Transduction of ECs and MIN6 Cells. CD31$^{-/-}$ ECs and MIN6 cells were seeded in six-well plates and cultured in DMEM to 60–70% confluence. Lentivirus was added to the cells in the presence of 5 μg/mL Polybrene (Sigma-Aldrich), and the six-well plate was centrifuged at 2,300 rpm (Heraeus Multifuge X3R, rotor Thermo Scientific 75003607) for 90 min at room temperature, followed by 8 h incubation at 37 °C with 5% CO_2. Virus was removed 24 h later; T cells were washed twice with PBS and incubated for 24 h in complete DMEM. Expression of GFP enabled tracking and sorting of infected cells by flow cytometry.

Skin Grafting. Skin grafting was performed using a method previously described by Billingham and Medawar (54) using tail skin grafted onto the lateral thorax. Briefly, donor tail skin was removed and cut into 1-cm^2 sections. Recipient mice were anesthetized using isoflurane (Halocarbon Products Corp.). A piece of skin was removed from the right flank to create a graft bed, and a 1-cm^2 piece of tail skin was placed in the graft bed. The graft was covered with muslin, and a plaster cast was wrapped around the midriff and graft. Plasters were removed 7–10 d after grafting, and grafts were inspected every other day.

Transplantation of Pancreatic β Cells. The recipient mice were anesthetized with pentobarbital sodium at 50 mg/kg and were placed in anatomical microscope. Then 5 × 10^5 β cells transfected for 6 min with the pWPT plasmid expressing CD31 or GFP were collected and grafted into the capsule of the left kidney of the recipient mice. One hundred microliters of Vetergesic Multidose (0.3 mg/mL) (Alstoe Animal Health) were given for postoperative analgesia.

Statistical Analysis. Results are expressed as mean ± SD or SEM, as indicated. The Student's *t* test and ANOVA were used. All reported *P* values are two-sided. A *P* value of less than 0.05 was regarded as significant.

1. Al-Lamki RS, Bradley JR, Pober JS (2008) Endothelial cells in allograft rejection. *Transplantation* 86(10):1340–1348.
2. Hesser BA, et al. (2004) Down syndrome critical region protein 1 (DSCR1), a novel VEGF target gene that regulates expression of inflammatory markers on activated endothelial cells. *Blood* 104(1):149–158.
3. Murphy TL, Murphy KM (2010) Slow down and survive: Enigmatic immunoregulation by BTLA and HVEM. *Annu Rev Immunol* 28:389–411.
4. LaGier AJ, Pober JS (2006) Immune accessory functions of human endothelial cells are modulated by overexpression of B7-H1 (PDL1). *Hum Immunol* 67(8):568–578.
5. Kaufmann SH, Hengartner MO (2001) Programmed cell death: Alive and well in the new millennium. *Trends Cell Biol* 11(12):526–534.
6. Affara M, et al. (2007) Understanding endothelial cell apoptosis: What can the transcriptome, glycome and proteome reveal? *Philos Trans R Soc Lond B Biol Sci* 362(1484):1469–1487.
7. Aoudjit F, Vuori K (2001) Matrix attachment regulates Fas-induced apoptosis in endothelial cells: A role for c-flip and implications for anoikis. *J Cell Biol* 152(3):633–643.
8. Ferrero E, et al. (2003) Transendothelial migration leads to protection from starvation-induced apoptosis in CD34+CD14+ circulating precursors: Evidence for PECAM-1 involvement through Akt/PKB activation. *Blood* 101(1):186–193.
9. Limaye V, et al. (2005) Sphingosine kinase-1 enhances endothelial cell survival through a PECAM-1-dependent activation of PI-3K/Akt and regulation of Bcl-2 family members. *Blood* 105(8):3169–3177.
10. Bannerman DD, et al. (2001) A constitutive cytoprotective pathway protects endothelial cells from lipopolysaccharide-induced apoptosis. *J Biol Chem* 276(18):14924–14932.
11. Muller WA (2003) Leukocyte-endothelial-cell interactions in leukocyte transmigration and the inflammatory response. *Trends Immunol* 24(6):327–334.
12. Jackson DE, Kupcho KR, Newman PJ (1997) Characterization of phosphotyrosine binding motifs in the cytoplasmic domain of platelet/endothelial cell adhesion molecule-1 (PECAM-1) that are required for the cellular association and activation of the protein-tyrosine phosphatase, SHP-2. *J Biol Chem* 272(40):24868–24875.
13. Newman PJ, Newman DK (2003) Signal transduction pathways mediated by PECAM-1: New roles for an old molecule in platelet and vascular cell biology. *Arterioscler Thromb Vasc Biol* 23(6):953–964.
14. Duncan GS, et al. (1999) Genetic evidence for functional redundancy of Platelet/Endothelial cell adhesion molecule-1 (PECAM-1): CD31-deficient mice reveal PECAM-1-dependent and PECAM-1-independent functions. *J Immunol* 162(5):3022–3030.
15. Graesser D, et al. (2002) Altered vascular permeability and early onset of experimental autoimmune encephalomyelitis in PECAM-1-deficient mice. *J Clin Invest* 109(3):383–392.
16. Tada Y, et al. (2003) Acceleration of the onset of collagen-induced arthritis by a deficiency of platelet endothelial cell adhesion molecule 1. *Arthritis Rheum* 48(11):3280–3290.
17. Ensminger SM, et al. (2002) Platelet-endothelial cell adhesion molecule-1 (CD31) expression on donor endothelial cells attenuates the development of transplant arteriosclerosis. *Transplantation* 74(9):1267–1273.
18. Carrithers M, et al. (2005) Enhanced susceptibility to endotoxic shock and impaired STAT3 signaling in CD31-deficient mice. *Am J Pathol* 166(1):185–196.
19. Maas M, et al. (2005) Endothelial cell PECAM-1 confers protection against endotoxic shock. *Am J Physiol Heart Circ Physiol* 288(1):H159–H164.
20. Gao C, et al. (2003) PECAM-1 functions as a specific and potent inhibitor of mitochondrial-dependent apoptosis. *Blood* 102(1):169–179.
21. Bergom C, Gao C, Newman PJ (2005) Mechanisms of PECAM-1-mediated cytoprotection and implications for cancer cell survival. *Leuk Lymphoma* 46(10):1409–1421.
22. Ashton-Rickardt PG (2010) Serine protease inhibitors and cytotoxic T lymphocytes. *Immunol Rev* 235(1):147–158.
23. Ma L, et al. (2010) Ig gene-like molecule CD31 plays a nonredundant role in the regulation of T-cell immunity and tolerance. *Proc Natl Acad Sci USA* 107(45):19461–19466.
24. Irmler M, et al. (1997) Inhibition of death receptor signals by cellular FLIP. *Nature* 388(6638):190–195.
25. Srinivasula SM, et al. (1997) FLAME-1, a novel FADD-like anti-apoptotic molecule that regulates Fas/TNFR1-induced apoptosis. *J Biol Chem* 272(30):18542–18545.
26. Zhang X, Tang N, Hadden TJ, Rishi AK (2011) Akt, FoxO and regulation of apoptosis. *Biochim Biophys Acta* 1813(11):1978–1986.
27. Park SJ, Sohn HY, Yoon J, Park SI (2009) Down-regulation of FoxO-dependent c-FLIP expression mediates TRAIL-induced apoptosis in activated hepatic stellate cells. *Cell Signal* 21(10):1495–1503.
28. Miyazaki J, et al. (1990) Establishment of a pancreatic beta cell line that retains glucose-inducible insulin secretion: Special reference to expression of glucose transporter isoforms. *Endocrinology* 127(1):126–132.
29. Valujskikh A, Lantz O, Celli S, Matzinger P, Heeger PS (2002) Cross-primed CD8(+) T cells mediate graft rejection via a distinct effector pathway. *Nat Immunol* 3(9):844–851.
30. Cavanagh G, Chapman CE, Carter V, Dickinson AM, Middleton PG (2005) Donor CD31 genotype impacts on transplant complications after human leukocyte antigen-matched sibling allogeneic bone marrow transplantation. *Transplantation* 79(5):602–605.
31. Dalmasso AP, et al. (2014) Interleukin-4 induces up-regulation of endothelial cell claudin-5 through activation of FoxO1: Role in protection from complement-mediated injury. *J Biol Chem* 289(2):838–847.
32. Kishore M, Ma L, Cornish G, Nourshargh S, Marelli-Berg FM (2012) Primed T cell responses to chemokines are regulated by the immunoglobulin-like molecule CD31. *PLoS One* 7(6):e39433.
33. Ma L, et al. (2012) CD31 exhibits multiple roles in regulating T lymphocyte trafficking in vivo. *J Immunol* 189(8):4104–4111.
34. Ilan N, Mohsenin A, Cheung L, Madri JA (2001) PECAM-1 shedding during apoptosis generates a membrane-anchored truncated molecule with unique signaling characteristics. *FASEB J* 15(2):362–372.
35. Fornasa G, et al. (2010) TCR stimulation drives cleavage and shedding of the ITIM receptor CD31. *J Immunol* 184(10):5485–5492.
36. Streilein JW (1995) Unraveling immune privilege. *Science* 270(5239):1158–1159.
37. Griffith TS, Brunner T, Fletcher SM, Green DR, Ferguson TA (1995) Fas ligand-induced apoptosis as a mechanism of immune privilege. *Science* 270(5239):1189–1192.
38. Bellgrau D, et al. (1995) A role for CD95 ligand in preventing graft rejection. *Nature* 377(6550):630–632.
39. Caligiuri G, et al. (2005) Reduced immunoregulatory CD31+ T cells in the blood of atherosclerotic mice with plaque thrombosis. *Arterioscler Thromb Vasc Biol* 25(8):1659–1664.
40. Fornasa G, et al. (2012) A CD31-derived peptide prevents angiotensin II-induced atherosclerosis progression and aneurysm formation. *Cardiovasc Res* 94(1):30–37.
41. Auer J, et al. (2003) Genetic polymorphisms in cytokine and adhesion molecule genes in coronary artery disease. *Am J Pharmacogenomics* 3(5):317–328.
42. Elrayess MA, et al. (2004) R643G polymorphism in PECAM-1 influences transendothelial migration of monocytes and is associated with progression of CHD and CHD events. *Atherosclerosis* 177(1):127–135.
43. Listì F, et al. (2004) Association between platelet endothelial cellular adhesion molecule 1 (PECAM-1/CD31) polymorphisms and acute myocardial infarction: A study in patients from Sicily. *Eur J Immunogenet* 31(4):175–178.
44. Listì F, et al. (2007) PECAM-1/CD31 in infarction and longevity. *Ann N Y Acad Sci* 1100:132–139.
45. Behar E, et al. (1996) Polymorphism of adhesion molecule CD31 and its role in acute graft-versus-host disease. *N Engl J Med* 334(5):286–291.
46. Balduini CL, et al. (2001) Donor-recipient incompatibility at CD31-codon 563 is a major risk factor for acute graft-versus-host disease after allogeneic bone marrow transplantation from a human leucocyte antigen-matched donor. *Br J Haematol* 114(4):951–953.
47. El-Chennawi FA, Kamel HA, Mosaad YM, El-Sherbini SM, El-Billey NA (2006) Impact of CD31 mismatches on the outcome of hematopoeitic stem cell transplant of HLA-identical sibling. *Hematology* 11(4):227–234.
48. Goodman RS, et al. (2005) Donor CD31 genotype and its association with acute graft-versus-host disease in HLA identical sibling stem cell transplantation. *Bone Marrow Transplant* 36(2):151–156.
49. Grumet FC, et al.; Brown BWM (2001) CD31 mismatching affects marrow transplantation outcome. *Biol Blood Marrow Transplant* 7(9):503–512.
50. Sahebkar A, Morris DR, Biros E, Golledge J (2013) Association of single nucleotide polymorphisms in the gene encoding platelet endothelial cell adhesion molecule-1 with the risk of myocardial infarction: A systematic review and meta-analysis. *Thromb Res* 132(2):227–233.
51. Marelli-Berg FM, Peek E, Lidington EA, Stauss HJ, Lechler RI (2000) Isolation of endothelial cells from murine tissue. *J Immunol Methods* 244(1-2):205–215.
52. Millrain M, et al. (2005) Identification of the immunodominant HY H2-D(k) epitope and evaluation of the role of direct and indirect antigen presentation in HY responses. *J Immunol* 175(11):7209–7217.
53. Jarmin SJ, et al. (2008) T cell receptor-induced phosphoinositide-3-kinase p110delta activity is required for T cell localization to antigenic tissue in mice. *J Clin Invest* 118(3):1154–1164.
54. Billingham R, Medawar PB (1951) The technique of free skin grafting in mammals. *J Exp Biol* 28:385–402.